Eur. Phys. J. C 30, 487–496 (2003)
Digital Object Identifier (DOI) 10.1140/epjc/s2003-01297-x

THE EUROPEAN PHYSICAL JOURNAL C

Transverse muon polarization in $K^+ \to \mu^+\nu_\mu\gamma$: scanning over the Dalitz plot

F.L. Bezrukov[a], D.S. Gorbunov[b], Yu.G. Kudenko[c]

Institute for Nuclear Research of the Russian Academy of Sciences, 60th October Anniversary prospect 7a, Moscow 117312, Russia

Received: 7 May 2003 / Revised version: 27 June 2003 /
Published online: 5 September 2003 –

Abstract. We study the potential of the measurement of the transverse muon polarization $P_{\rm T}$ in the $K \to \mu\nu_\mu\gamma$ decay with a sensitivity of $\delta P_{\rm T} \sim 10^{-4}$. It is shown that the forthcoming experiment can measure the contribution of the electromagnetic final state interactions to $P_{\rm T}$ that gives a possibility to unambiguously determine the signs of the sum of the kaon form factors $F_{\rm V}$ and $F_{\rm A}$ even without fixing their difference. We also estimate the sensitivity of this experiment to the new physics, which could give rise to T-violation: multi-Higgs doublet models, supersymmetric extensions of the Standard Model, left–right symmetric model and leptoquark models.

1 Introduction

In spite of remarkable progress in the study of CP-violation phenomena in both K and B sector there remains an interesting issue. The Standard Model (SM) successfully describes existing experimental data by a single phase of the CKM matrix, although it is hard to believe that this phase is the only source of CP-violation. For example, the baryon asymmetry of the universe cannot be explained by the CKM phase only, and at least one additional source of CP-violation is required.

A good place to look for new CP-violating phases is a measurement of processes where the SM CP-violation is vanishing or very suppressed, while additional or alternative sources of CP-violation can produce a sizable effect. Such interesting observables are the electric dipole moment of the neutron, which is extremely small in the SM, and the transverse lepton polarization in three-body decays of kaons and B-mesons [1–3].

In this paper, we study the T-odd muon polarization in the decay $K^+ \to \mu^+\nu_\mu\gamma$ ($K_{\mu 2\gamma}$). Namely, we investigate the possibility to measure the vector and axial-vector kaon form factors, $F_{\rm V}$ and $F_{\rm A}$, from the T-odd muon polarization emerging due to the electromagnetic final state interactions (FSI). Also we analyze potential contributions to $P_{\rm T}$ from various extensions of the SM. In this study we focus on the Dalitz plot region where $K_{\mu 2\gamma}$ events have a large angle between photon and muon momenta. This is the region where T-odd muon polarization exhibits the best sensitivity to $F_{\rm V}$ and $F_{\rm A}$. Moreover, we found that in this region the ratio of the possible contribution to $P_{\rm T}$ from new physics and the FSI contribution to $P_{\rm T}$ becomes the largest. Hence, the analysis of the $K_{\mu 2\gamma}$ events at large θ will provide the best accuracy in the measurement of the relevant parameters of the new physics or the strongest constraints on them.

It is found that the $P_{\rm T}$ dependence on the kaon form factors gives a possibility to unambiguously determine in $K_{\mu 2\gamma}$ decay the signs of the sum of the kaon form factors without fixing their difference. Combined with a measurement of the normal muon polarization, which is very sensitive to $F_{\rm V}$ and $F_{\rm A}$ [13], this allows the values of the kaon form factors to be unambiguously extracted with 1% accuracy from this experiment. Investigating the prospects of new experiments in searching for new physics we show that, generally, they are limited mostly by the uncertainty in FSI predictions rather than by the anticipated statistical error.

The outline of this paper is as follows. In Sect. 2 we introduce the parameters describing the muon transverse polarization $P_{\rm T}$ in the $K_{\mu 2\gamma}$ decay, recall the relevant formulae and estimate the expected sensitivity to $P_{\rm T}$ in forthcoming experiments. In Sect. 3, an approach to determine the signs of the sum of the kaon form factors from the FSI polarization is discussed and the accuracy of this method is estimated. In Sect. 4 we study in general the discovery potential of the $P_{\rm T}$ measurements in the search for new physics. Using this analysis, we estimate in Sect. 5 the upper bounds on the $P_{\rm T}$ in multi-Higgs doublet models, supersymmetric extensions of the Standard Model, left–right symmetric model and leptoquark models. Section 6 contains conclusions and final remarks.

[a] e-mail: fedor@ms2.inr.ac.ru
[b] e-mail: gorby@ms2.inr.ac.ru
[c] e-mail: kudenko@wocup.inr.troitsk.ru

2 Transverse muon polarization in $K_{\mu 2\gamma}$ decay

2.1 General description

Introducing the three unit vectors

$$\mathbf{e}_{\rm L} = \frac{\mathbf{p}_\mu}{|\mathbf{p}_\mu|}\,, \quad \mathbf{e}_{\rm N} = \frac{\mathbf{p}_\mu \times (\mathbf{q}\times\mathbf{p}_\mu)}{|\mathbf{p}_\mu \times (\mathbf{q}\times\mathbf{p}_\mu)|}\,, \quad \mathbf{e}_{\rm T} = \frac{\mathbf{q}\times\mathbf{p}_\mu}{|\mathbf{q}\times\mathbf{p}_\mu|}\,,$$

with p_μ and q being the four-momenta of μ^+ and γ, respectively, one can define longitudinal ($P_{\rm L}$), normal ($P_{\rm N}$) and transverse ($P_{\rm T}$) components of the muon polarization as the corresponding contributions to the squared matrix element of the $K_{\mu 2\gamma}$ decay,

$$|M|^2 = \rho_0\big[1 + (P_{\rm L}\mathbf{e}_{\rm L} + P_{\rm N}\mathbf{e}_{\rm N} + P_{\rm T}\mathbf{e}_{\rm T})\cdot\boldsymbol{\xi}\big]\,,$$

with $\boldsymbol{\xi}$ being a unit vector along the muon spin, and ρ_0 is

$$\rho_0(x,y) = \frac{1}{2}e^2 G_{\rm F}^2 |V_{us}|^2 (1-\lambda) \times \big\{f_{\rm IB}(x,y) + f_{\rm SD}(x,y) + f_{\rm IBSD}(x,y)\big\}\,,$$

where the internal bremsstrahlung (IB), structure dependent (SD) and interference contributions (IBSD) are given by [3–5]

$$f_{\rm IB} = \frac{4m_\mu^2|f_K|^2}{\lambda x^2}\left[x^2 + 2(1-r_\mu)\left(1-x-\frac{r_\mu}{\lambda}\right)\right]\,, \quad (1)$$

$$f_{\rm SD} = m_K^4 x^2\bigg[|F_{\rm V}+F_{\rm A}|^2\frac{\lambda^2}{1-\lambda}\Big(1-x-\frac{r_\mu}{\lambda}\Big) + |F_{\rm V}-F_{\rm A}|^2(y-\lambda)\bigg]\,, \quad (2)$$

$$f_{\rm IBSD} = -4m_K m_\mu^2\bigg[{\rm Re}[f_K(F_{\rm V}+F_{\rm A})^*]\left(1-x-\frac{r_\mu}{\lambda}\right) - {\rm Re}[f_K(F_{\rm V}-F_{\rm A})^*]\frac{1-y+\lambda}{\lambda}\bigg]\,. \quad (3)$$

Here we used the standard notation $\lambda = (x+y-1-r_\mu)/x$, $r_\mu = m_\mu^2/m_K^2$, and $x = 2E_\gamma/m_K$, $y = 2E_\mu/m_K$ with E_γ, E_μ being the photon and muon energies in the kaon rest frame, respectively; $G_{\rm F}$ is the Fermi constant, V_{us} is the corresponding element of the Cabibbo–Kobayashi–Maskawa (CKM) matrix and $f_K = 159.8\,{\rm MeV}$ is the kaon decay constant. In terms of these variables the differential decay width reads

$${\rm d}\Gamma(\boldsymbol{\xi}) = \frac{m_K}{32(2\pi)^3}|M(x,y,\xi)|^2 {\rm d}x\,{\rm d}y\,.$$

The transverse muon polarization $P_{\rm T}$ is determined using the partial decay width

$$P_{\rm T} = \frac{{\rm d}\Gamma(\mathbf{e}_{\rm T}) - {\rm d}\Gamma(-\mathbf{e}_{\rm T})}{{\rm d}\Gamma(\mathbf{e}_{\rm T}) + {\rm d}\Gamma(-\mathbf{e}_{\rm T})} \equiv \frac{\rho_{\rm T}}{\rho_0}\,. \quad (4)$$

This is a T-odd observable (both $P_{\rm L}$ and $P_{\rm N}$ are T-even); hence in the T-invariant theory its value equals zero at tree level. Moreover, $P_{\rm T}$ does not have tree-level contributions from the CP-violating phase in the CKM matrix. These two features make $P_{\rm T}$ a very promising observable for new CP-violating physics searches. At the same time, as will be seen in Sect. 3, the analysis of loop contributions from the Standard Model (FSI) is also of special physical interest.

2.2 Experimental sensitivity to $P_{\rm T}$

For the following analysis let us estimate the level of precision which could be achieved experimentally.

The running E246 experiment at KEK [6] dedicated to a measurement of $P_{\rm T}$ in the decay $K^+ \to \pi^0\mu^+\nu$ has only a limited sensitivity of about 10^{-2} to $P_{\rm T}$ in $K_{\mu 2\gamma}$ [7]. There is a proposal for a new experiment in which a statistical sensitivity $P_{\rm T} \le 10^{-4}$ in $K_{\mu 2\gamma}$ can be reached [8]. The main features of this experiment include a high resolution measurement of neutral particles from $K_{\mu 3}$ and $K_{\mu 2\gamma}$ decays, usage of an active muon polarimeter which provides information about stopped muons (stopping point, momentum), positron direction, and which also detects photons, and a highly efficient photon veto system covering nearly 4π solid angle. This approach allows one to accumulate $K_{\mu 2\gamma}$ events for all θ angles between photon and muon momenta due to the efficient photon veto detector. This system eliminates $K_{\pi 2}$ decays which are the main background source at large θ.

Using parameters of the proposed detector [8] and the kaon beam intensity of about 10^7 K^+ per second expected at the JHF [9] one can estimate the sensitivity to $P_{\rm T}$ which could be achieved in this experiment. With an analyzing power of the detector ~ 0.3 and a kinematical attenuation factor ~ 0.8, the expected sensitivity to $P_{\rm T}$ in some region $\mathcal{R}$ of the Dalitz plot can be expressed as

$$\delta P_{\rm T}(\mathcal{R}) \simeq \frac{1}{0.3\cdot 0.8\sqrt{N_{K_{\mu 2\gamma}}(\mathcal{R})}}\,, \quad (5)$$

where $N_{K_{\mu 2\gamma}}(\mathcal{R})$ is the number of $K_{\mu 2\gamma}$ events in the region $\mathcal{R}$. In this experiment, the most effective suppression of background events is anticipated to occur in the kinematic region with $E_\gamma > 20\,{\rm MeV}$, $E_\mu > 200\,{\rm MeV}$. There the number of $K_{\mu 2\gamma}$ events accumulated for one year running period is estimated to be 3×10^{10}. In what follows we adopt these cuts as well as the number of events.

The branching ratio of this decay for $E_\gamma > 20\,{\rm MeV}$ and $E_\mu > 200\,{\rm MeV}$ integrated over 10° wide bins in θ is presented in Fig. 1. From this plot one can estimate the sensitivity to $P_{\rm T}$ in various θ regions.

3 FSI and pinning down the kaon form factors

3.1 Predictions and experimental data

Due to lack of understanding of the QCD low-energy structure, there is no definite prediction for the values of the $F_{\rm V}$ and $F_{\rm A}$ form factors: the calculation of these is a model dependent procedure. So the measurement of these form

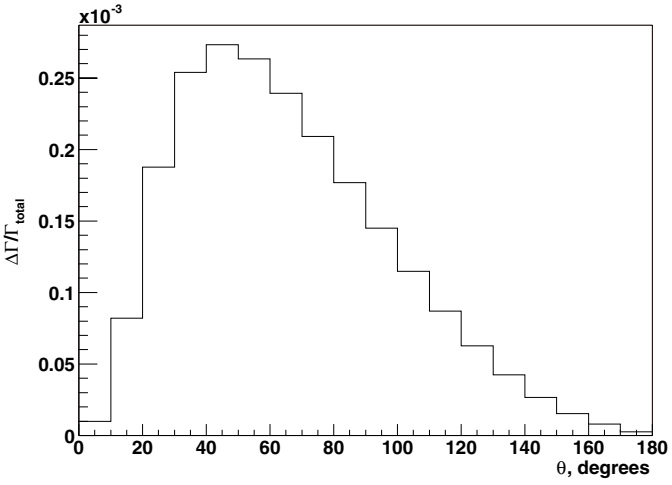

Fig. 1. Branching ratio for $K_{\mu 2\gamma}$ decay for 10° wide bins in θ; $E_\gamma > 20\,\mathrm{MeV}$, $E_\mu > 200\,\mathrm{MeV}$. The dependence of this branching ratio on the values of the F_V, F_A form factors is quite weak

factors would give a possibility to make a choice between various candidates for the correct description of the QCD low-energy limit.

The distribution of the $K_{\mu 2\gamma}$ decay width over the Dalitz plot allows only the absolute values of the sum and difference of the kaon form factors to be measured, since the term f_IBSD (see (3)) is small. The terms with a linear and quadratic dependence on F_V and F_A give a comparable contribution in some regions of the Dalitz plot that could, in principle, make it possible to measure the signs as well as the magnitudes of the form factors. Unfortunately, in the region where the linear terms grow, the dominant contribution to $K_{\mu 2\gamma}$ (internal bremsstrahlung; see (1), which depends only on f_K) also increases. That significantly reduces the sensitivity of Dalitz plot measurements to the kaon form factors. In practice, the situation is even worse, since only the absolute value of the sum of the kaon form factors has been measured with good accuracy in these measurements, while their difference still has only lower and upper bounds [10, 11]:

$$|F_\mathrm{V} + F_\mathrm{A}| = 0.165 \pm 0.013\,, \tag{6}$$

$$-0.24 < F_\mathrm{A} - F_\mathrm{V} < 0.04\,. \tag{7}$$

Recently, both vector and axial-vector form factors have been measured in $K^+ \to \mu^+\nu_\mu e^+e^-$ and $K^+ \to e^+\nu_e e^+e^-$ decays [12]. These decays are generalizations of $K_{l2\gamma}$ for the case of a virtual photon in the final state, so the kaon form factors F_V and F_A are believed to be the same in all these processes. The combined fit for both four-body decay experiments results in

$$F_\mathrm{V} = -0.112 \pm 0.018\,, \qquad F_\mathrm{A} = -0.035 \pm 0.020\,. \tag{8}$$

These values are in a good agreement with $\mathcal{O}\left(p^4\right)$ predictions [4, 14] of the chiral perturbation theory (ChPT):

$$F_\mathrm{V} = -0.096\,, \qquad F_\mathrm{A} = -0.041 \pm 0.006\,. \tag{9}$$

3.2 Dependence on Q^2

It is worth to note that actually F_V and F_A are not constants, but some functions of the momentum of the lepton pair, $Q^2 \equiv (p_K - q)^2$, with p_K being the kaon four-momentum. In ChPT the Q^2 dependence emerges due to higher order corrections, which have not been calculated yet. Their magnitude can be estimated to be

$$\frac{\Delta F_{\mathrm{V,A}}}{F_{\mathrm{V,A}}} \sim \frac{Q^2}{m^2_{\mathrm{V,A}}} = (1-x)\frac{m_K^2}{m^2_{\mathrm{V,A}}}\,,$$

where m_V and m_A are masses of the first strange hadronic vector (K^*) and axial-vector (K_1) resonances, respectively. This estimate implies corrections as large as 25%; hence the experimental data on $K_{l2\gamma}$ should be fitted with at least two additional parameters, which generally decreases the chances to determine F_V and F_A in $K_{l2\gamma}$ experiments.

In $K^+ \to l^+\nu_l e^+e^-$ both vector and axial-vector form factors get an additional dependence on the non-zero q^2 that also increases the bias in the corresponding fitting procedure. In [12] the experimental data were fitted assuming constant form factors and form factors depending on Q^2 and q^2,

$$F_{\mathrm{V,A}}(Q^2, q^2) = \frac{F_{\mathrm{V,A}}}{(1 - q^2/m_\rho^2)(1 - Q^2/m^2_{\mathrm{V,A}})}\,, \tag{10}$$

with m_ρ being the mass of the ρ meson. This dependence appears in the approximation of dominance of the contribution of the lowest lying resonances [14]. The experimental data favor the dependence (10) over the constant $F_{\mathrm{V,A}}$, though the accuracy achieved in this experiment did not allow a definite confirmation or rejection to be reached of the Q^2, q^2 dependence.

The determination of the Q^2 dependence of the form factors may be done in future experiments. In particular, an analysis of the P_N muon polarization in $K_{\mu 2\gamma}$ decays can improve our knowledge of the $F_{\mathrm{V,A}}$ behavior for sure [13]. However, at present, the unknown Q^2 dependence imports some uncertainty into the predictions for the muon asymmetry to be measured in future experiments. This concerns an FSI contribution as well as a possible contribution from new physics, since both are functions of the kaon form factors.

To avoid all these difficulties one can try to find a physical observable which strongly depends on F_V and F_A and can be measured with an accuracy sufficient to distinguish the signs of kaon form factors in the $K_{\mu 2\gamma}$ decay. This implies that

(i) the observable we are interested in should exhibit a linear dependence on F_V and F_A in some region of the Dalitz plot;

(ii) in this region the differential partial width should be sufficiently large;

(iii) the Q^2-corrections in this region should be small enough to unambiguously determine the sign of the kaon form factors.

Below we consider the transverse muon polarization calculated in the framework of the Standard Model as a physical observable, which pins down the signs of kaon form factors in $K_{\mu 2\gamma}$ decay.

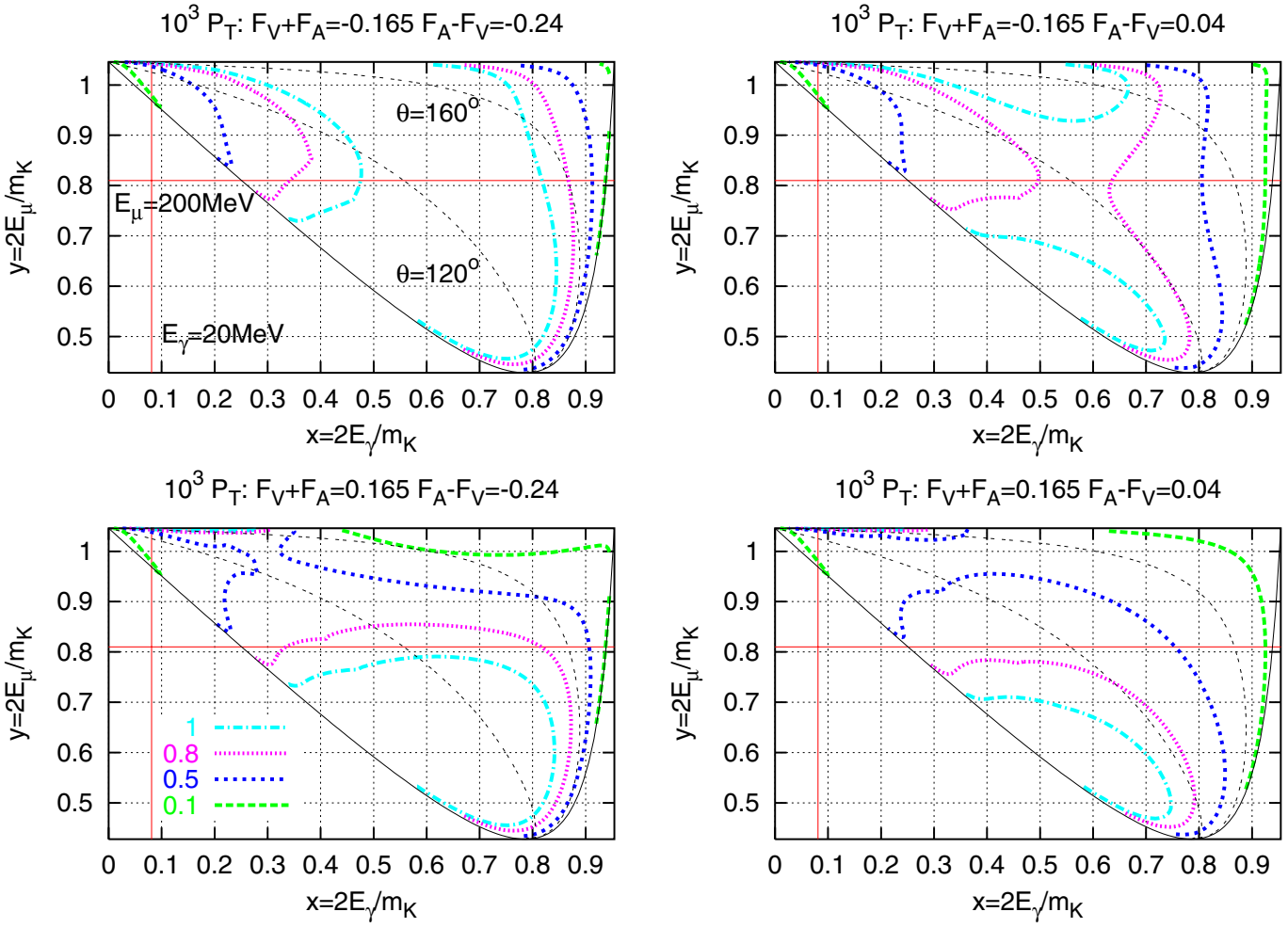

Fig. 2. $P_{\rm T}$ distribution for different $F_{\rm V}+F_{\rm A}$ and $F_{\rm A}-F_{\rm V}$ values. The imposed cuts $E_\gamma > 20$MeV, $E_\mu > 200$MeV and the region $120^\circ < \theta < 160^\circ$ are also shown

3.3 Final state interactions

In the framework of the Standard Model, the contribution to $P_{\rm T}$ emerges only at loop levels due to the FSI. This contribution has recently been calculated [15] at one-loop level. The expression for $\rho_{\rm T}^{\rm SM}(x,y)$ can be read from [15] after changing the definitions of the form factors: $F_{\rm V}^{\text{Ref. [15]}} \to -m_K F_{\rm V}$ and $F_{\rm A}^{\text{Ref. [15]}} \to m_K F_{\rm A}$. The asymmetry is positive at any relevant (x,y) and its absolute value ranges from zero to 1.5×10^{-3}. The Dalitz plot distribution of $P_{\rm T}$ for several values of the form factors satisfying (6) and (7) is presented in Fig. 2.

3.4 Experimental prospects for the determination of the form factors

The transverse muon polarization emerging from the FSI exhibits the behavior we are looking for to pin down the signs of the kaon form factors. Indeed, the muon transverse polarization is sensitive to the signs of $F_{\rm V}$ and $F_{\rm A}$, especially at large angles θ between photon and muon momenta.

To illustrate this point we present the $P_{\rm T}$ values integrated over 10° intervals as a function of θ in Fig. 3. The value of $P_{\rm T}$ associated with a bin $\theta_1 < \theta < \theta_2$ is determined by

$$P_{\rm T}(\theta_1<\theta<\theta_2) = \frac{\int\limits_{\text{cuts},\,\theta_1<\theta<\theta_2} \rho_{\rm T}\,{\rm d}x\,{\rm d}y}{\int\limits_{\text{cuts},\,\theta_1<\theta<\theta_2} \rho_0\,{\rm d}x\,{\rm d}y}\,, \qquad (11)$$

where the additional relevant cuts are $E_\gamma > 20\,$MeV, $E_\mu > 200\,$MeV. We evaluate $P_{\rm T}$ for four different sets of form factors corresponding to the boundaries of the allowed intervals (6) and (7). One can see that the predictions for $P_{\rm T}$ differ significantly, and in the region of large angles, $\theta > 120^\circ$, the sign of $F_{\rm V}+F_{\rm A}$ can be unambiguously determined from the $P_{\rm T}$ analysis *only*. Suppression of the $K_{\pi 2}$ decays becomes less efficient at very large θ angles because of the low efficiency of the detection of low-energy photons from asymmetrical π^0 decays, so we adopt the region $120^\circ < \theta < 160^\circ$ as the realistic region with the best sensitivity to the kaon form factors. The difference between the $P_{\rm T}$ values increases with θ and reaches its maximum value at $\theta \sim 150^\circ$, as seen from Fig. 3. Although

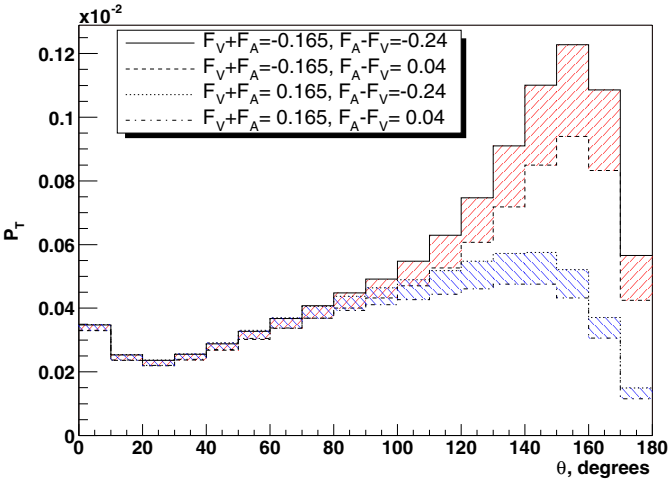

Fig. 3. $P_{\rm T}$ (FSI) asymmetry for 10° wide bins in θ. The upper region corresponds to negative $F_{\rm V}+F_{\rm A}$ and the lower one to positive values

the differential $K_{\mu2\gamma}$ branching ratio decreases at large θ, its value is still reasonable at large θ; see Fig. 1. The fraction of the $K_{\mu2\gamma}$ events within $120^\circ < \theta < 160^\circ$ is about 7%. By making use of (5), the statistical sensitivity to $P_{\rm T}$ in this Dalitz plot region is estimated to be

$$\delta P_{\rm T}(120^\circ < \theta < 160^\circ) \sim 1.0 \times 10^{-4}\,, \quad 1\sigma \text{ level.} \qquad (12)$$

To unambiguously determine the sign of $F_{\rm V}+F_{\rm A}$ without any additional data on the difference of the form factors, one has to be able to distinguish the $P_{\rm T}$ values with $F_{\rm V}+F_{\rm A}=0.165$, $F_{\rm A}-F_{\rm V}=-0.24$ and $F_{\rm V}+F_{\rm A}=-0.165$, $F_{\rm A}-F_{\rm V}=0.04$ (the two closest lines in Fig. 3). For these two sets of form factors, the difference between $P_{\rm T}$ values in the region $120^\circ < \theta < 160^\circ$ is 1.6×10^{-4}, which allows a determination to be made of the sign of the sum of the form factors at the level of 1.6σ. Note that there is no usual degeneracy related to the signs of the sum of the form factors, that provides a possibility to pin down the sign of the sum without fixing the difference.

If the difference between the form factors is measured with a better precision than in (7) one has to compare the situations with equal $F_{\rm A}-F_{\rm V}$ and different signs of the sum of the form factors, that gives the difference in $P_{\rm T}$ values in the same region ($120^\circ < \theta < 160^\circ$) of (2.6–3.6) $\times 10^{-4}$, depending on the precise value of $F_{\rm A}-F_{\rm V}$. Then the statistical sensitivity (12) allows one to determine the signs at the level of 3–4σ.

So measurement of $P_{\rm T}$ allows the signs of the form factors to be distinguished. It is worth to note in passing that at large θ the main contribution to the $P_{\rm T}$ (FSI) comes from the Dalitz plot region $x > 0.4$, where the uncertainty associated with the momentum of the lepton pair Q^2 is $\lesssim 15\%$. This uncertainty is small enough to be neglected, because it is significantly less than the difference in $P_{\rm T}$ for the form factors of different signs; see Fig. 3.

Recently we found [13] that the normal muon polarization $P_{\rm N}$ is extremely sensitive to the values of the form factors. Since measurement of $P_{\rm T}$ pins down the sign of the form factors, it will provide a possibility of an independent cross-check of the results from the measurement of $P_{\rm N}$ in the future experiment [8], which will determine $F_{\rm V}$ and $F_{\rm A}$ with an accuracy as high as 1% [13] based only on its own experimental data.

4 New physics: general analysis

4.1 Standard parameterization

For a general investigation of the possible contribution of some new CP-violating sources to the transverse muon polarization in $K_{\mu2\gamma}$ we first introduce the most general four-fermion interaction

$$\begin{aligned}\mathcal{L} = &-\frac{G_{\rm F}}{\sqrt{2}}V_{us}^*\bar{s}\gamma^\alpha(1-\gamma_5)u\cdot\bar{\nu}\gamma_\alpha(1-\gamma_5)\mu\\ &+G_{\rm V}\bar{s}\gamma^\alpha u\cdot\bar{\nu}\gamma_\alpha(1-\gamma_5)\mu+G_{\rm A}\bar{s}\gamma^\alpha\gamma_5 u\cdot\bar{\nu}\gamma_\alpha(1-\gamma_5)\mu\\ &+G_{\rm S}\bar{s}u\cdot\bar{\nu}(1+\gamma_5)\mu+G_{\rm P}\bar{s}\gamma_5 u\cdot\bar{\nu}(1+\gamma_5)\mu+\text{h.c.}\,,\end{aligned}$$

where $G_{\rm S}$, $G_{\rm P}$, $G_{\rm V}$, and $G_{\rm A}$, arising from new physics, denote scalar, pseudoscalar, vector, and axial-vector coupling constants, respectively. Their contribution to the $K_{\mu2\gamma}$ decay amplitude may be taken into account by the redefinition of the usual kaon form factors as follows:

$$\begin{aligned}f_K &\to f_K\,(1+\Delta_{\rm P}+\Delta_{\rm A})\,,\\ F_{\rm V} &\to F_{\rm V}(1+\Delta_{\rm V}),\\ F_{\rm A} &\to F_{\rm A}(1-\Delta_{\rm A}),\end{aligned}$$

with

$$\Delta_{\rm (P,A,V)} = \frac{\sqrt{2}}{G_{\rm F}V_{us}^*}\left(\frac{G_{\rm P}B_0}{m_\mu}, G_{\rm A}, G_{\rm V}\right).$$

The constant B_0 is related to the quark condensate as $\langle 0|\bar{q}q|0\rangle = -\frac{1}{2}B_0 f_{\pi^0}^2$ and may be evaluated from the masses of kaon and quarks, $B_0 = M_{K^0}^2/(m_d+m_s) \approx 2\,\text{GeV}$. The scalar-type interaction $G_{\rm S}$ does not contribute to $K_{\mu2\gamma}$ decay because of parity, and will not be considered below. Note, however, that it contributes to the transverse muon polarization in the $K\to\pi^0\mu\nu_\mu$ ($K_{\mu3}$) decays (while the pseudoscalar interaction $G_{\rm P}$ does not).

The imaginary parts of the new coupling constants are responsible for CP-violation and could give rise to tree-level contributions to the muon polarization [3–5],

$$\begin{aligned}\rho_{\rm T}(x,y) = &-2e^2G_{\rm F}^2|V_{us}|^2m_K^2m_\mu\frac{1-\lambda}{\lambda}\sqrt{\lambda y-\lambda^2-r_\mu}\\ &\times\left\{\text{Im}\left[f_K(F_{\rm V}+F_{\rm A})^*\right]\frac{\lambda}{1-\lambda}\times\left(1-x-\frac{r_\mu}{\lambda}\right)\right.\\ &\left.+\,\text{Im}\left[f_K(F_{\rm V}-F_{\rm A})^*\right]\right\}.\end{aligned}$$

It is convenient to rewrite $P_{\rm T}(x,y)$ as

$$P_{\rm T}(x,y) = P_{\rm T}^{\rm V}(x,y) + P_{\rm T}^{\rm A}(x,y)\,,$$

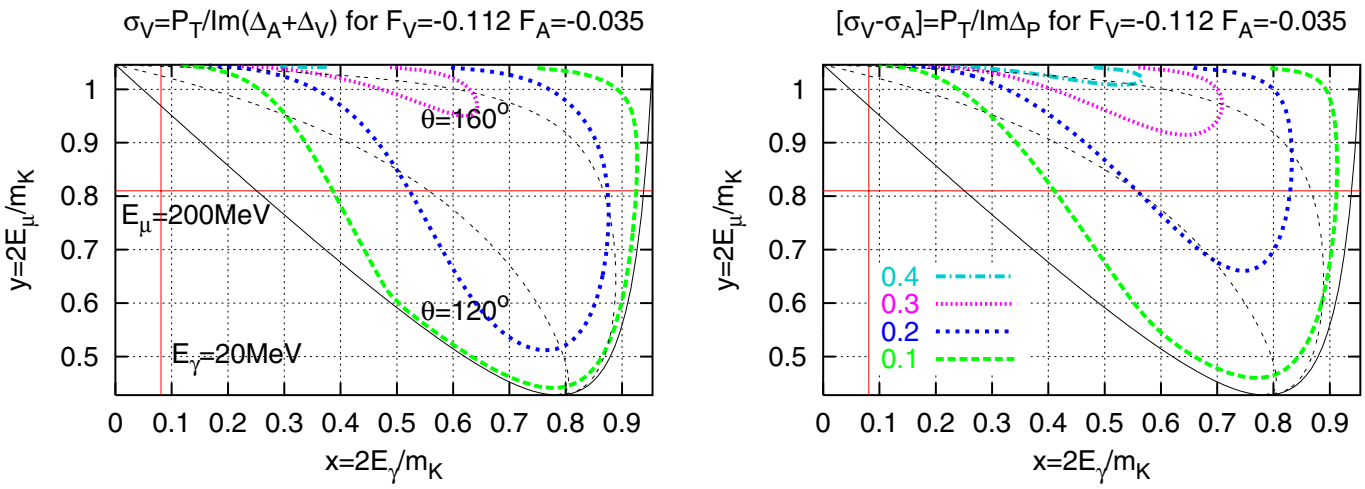

Fig. 4. Distribution of $\sigma_{\rm V}$ and $[\sigma_{\rm V} - \sigma_{\rm A}]$ over the Dalitz plot

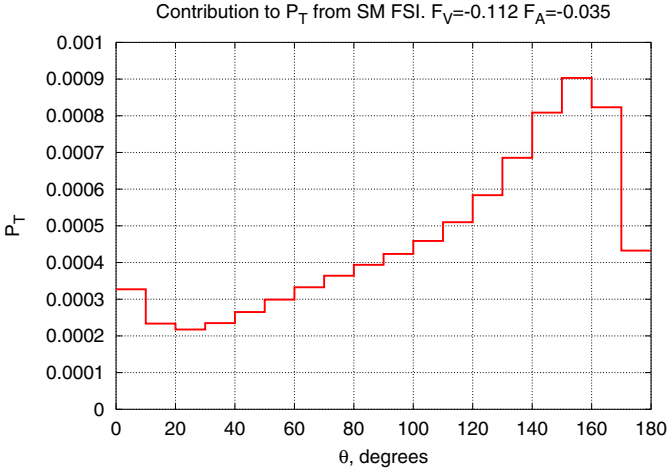

Fig. 5. FSI contribution to $P_{\rm T}$ for 10° wide bins in θ; the kaon form factors are equal to the measured values (8)

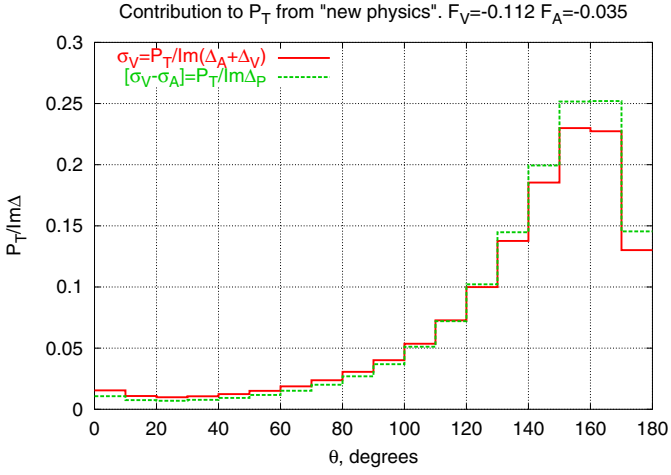

Fig. 6. $P_{\rm T}$ for 10° wide bins in θ at $\mathrm{Im}(\Delta_{\rm V}+\Delta_{\rm A}) = \mathrm{Im}(\Delta_{\rm P}) = 1$; the kaon form factors are equal to the measured values (8)

with

$$P_{\rm T}^{\rm V}(x,y) = \sigma_{\rm V}(x,y)\mathrm{Im}(\Delta_{\rm A}+\Delta_{\rm V})\,,$$
$$P_{\rm T}^{\rm A}(x,y) = [\sigma_{\rm V}(x,y) - \sigma_{\rm A}(x,y)]\,\mathrm{Im}(\Delta_{\rm P})\,, \qquad (13)$$

where

$$\sigma_{\rm V}(x,y) = 2e^2G_{\rm F}^2|V_{us}|^2m_K^2m_\mu f_K F_{\rm V} \times \frac{\sqrt{\lambda y-\lambda^2-r_\mu}}{\rho_0(x,y)}\left[\frac{\lambda-1}{\lambda} - \left(1-x-\frac{r_\mu}{\lambda}\right)\right],$$

$$\sigma_{\rm A}(x,y) = 2e^2G_{\rm F}^2|V_{us}|^2m_K^2m_\mu f_K F_{\rm A} \times \frac{\sqrt{\lambda y-\lambda^2-r_\mu}}{\rho_0(x,y)}\left[\frac{\lambda-1}{\lambda} + \left(1-x-\frac{r_\mu}{\lambda}\right)\right].$$

4.2 Distribution over the Dalitz plot

To illustrate the sensitivity of the transverse muon polarization to new physics we adopt the experimental values (8) for the kaon form factors and plot the $P_{\rm T}$ values integrated over 10° θ intervals as a function of θ (see the definition (11)) in Fig. 5. The distributions of $P_{\rm T}^{\rm V}$ and $P_{\rm T}^{\rm A}$ over the Dalitz plot are completely determined by the functions $\sigma_{\rm V}(x,y)$ and $[\sigma_{\rm V}(x,y) - \sigma_{\rm A}(x,y)]$, presented in Fig. 4. Indeed, the values of new CP-violating coupling constants provide only the normalization factors; see (13). To understand the general behavior we present $P_{\rm T}^{\rm V}$ and $P_{\rm T}^{\rm A}$ values for 10° wide bins in θ at $\mathrm{Im}(\Delta_{\rm V}+\Delta_{\rm A}) = \mathrm{Im}(\Delta_{\rm P}) = 1$ in Fig. 6.

Comparing Figs. 5 and 6 one can realize that while both FSI and new physics contributions are peaked at large θ, the slope is steeper in the former case:

$$\frac{P_{\rm T}^{\rm V}(\theta\sim 150^\circ)}{P_{\rm T}^{\rm V}(\theta\sim 20^\circ)} \simeq 20\,, \quad \frac{P_{\rm T}^{\rm A}(\theta\sim 150^\circ)}{P_{\rm T}^{\rm A}(\theta\sim 20^\circ)} \simeq 35\,, \qquad (14)$$

$$\frac{P_{\rm T}^{\rm FSI}(\theta\sim 150^\circ)}{P_{\rm T}^{\rm FSI}(\theta\sim 20^\circ)} \simeq 4.5\,. \qquad (15)$$

This shows that the sensitivity to new physics increases the region of the Dalitz plot with large θ angles. Indeed, the best way to distinguish FSI and new physics contributions is to compare the θ dependence and $P_{\rm T}$ averaged over the large angles, $\theta = 120°$–$160°$. For this range we obtain

$$P_{\rm T}^{\rm V}(120° < \theta < 160°) = 0.14 \cdot {\rm Im}(\Delta_{\rm V} + \Delta_{\rm A})\,, \quad (16)$$

$$P_{\rm T}^{\rm A}(120° < \theta < 160°) = 0.15 \cdot {\rm Im}(\Delta_{\rm P})\,. \quad (17)$$

Taking into account the expected experimental sensitivity (12) one may hope to detect effects of new physics leading to ${\rm Im}(\Delta_{\rm V} + \Delta_{\rm A})$ or ${\rm Im}\Delta_{\rm P}$ as small as 0.7×10^{-3} at 1σ level.

In the estimation of the sensitivity presented above we neglected the contribution to $P_{\rm T}$ from the FSI. This is possible if one reduces the uncertainty in the prediction of $P_{\rm T}^{\rm FSI}$ to values smaller than $\delta P_{\rm T}$. To this end a careful determination of the $F_{\rm A}$ and $F_{\rm V}$ form factors from other experiments is needed – for example, from $K \to l\nu_l e^+e^-$, see (8), or from the measurement of the normal muon polarization $P_{\rm N}$ in $K_{\mu 2\gamma}$ decay, which is also a very sensitive to the form factors observable [13]. Simultaneous measurement of both $P_{\rm N}$ and $P_{\rm T}$ in one experiment with the same statistical sensitivity provides a good opportunity for an accurate determination of $F_{\rm A}$ and $F_{\rm V}$ from $P_{\rm N}$ and, therefore, a precise calculation of the FSI contribution to the measured $P_{\rm T}$ and a clear separation of the non-SM $P_{\rm T}$ from the physics background.

The values of $\Delta_{\rm V}$, $\Delta_{\rm A}$ and $\Delta_{\rm P}$ are completely determined by the physics beyond the Standard Model. Below we consider several extensions of the SM and present the corresponding bounds on $\Delta_{\rm V}$, $\Delta_{\rm A}$ and $\Delta_{\rm P}$ from the existing experimental data.

5 New physics: possible models

5.1 Two-Higgs doublet models with suppressed FCNC

In a general two-Higgs doublet (2HD) model [1] up- and down-type quarks, as well as leptons, couple to both two-Higgs doublets. The up- and down-type quark mass matrices cannot be diagonalized simultaneously; that is the reason for the flavor changing neutral current to be induced at tree level. The relevant terms read [5]

$$\mathcal{L}_{\rm 2HD} = \frac{z m_\mu}{4M_H^2}\bar{s}\sum_i\left[\tilde{\xi}^{D*}_{i2}V^*_{ui}(1-\gamma_5) - \tilde{\xi}^{U*}_{i1}V^*_{is}(1+\gamma_5)\right]u \times\bar{\nu}(1+\gamma_5)\mu\,, \quad (18)$$

where M_H is the mass of the charged Higgs boson, $z m_{l_i}$ are the coupling constants of the charged Higgs boson and the corresponding leptons, and the $\tilde{\xi}^{U,D}_{ij}$ are the mixing matrices parameterizing up- and down-type quark interactions with the lightest neutral Higgs boson. This interaction results in the muon transverse polarization

$${\rm Im}\Delta_{\rm P} = -\frac{B_0 z}{2\sqrt{2}G_{\rm F}M_H^2|V_{us}|}\sum_i {\rm Im}\left[V^*_{is}\tilde{\xi}^U_{i1} + V^*_{ui}\tilde{\xi}^{D*}_{i2}\right]\,. \quad (19)$$

The measurement of $b \to s\gamma$ gives $M_H > 315\,{\rm GeV}$ [16]; the perturbativity bound (see, e.g., [17]) implies $z < 2\,{\rm GeV}^{-1}$. The constraint 19 depends greatly on the form of the mixing matrices $\tilde{\xi}^{U,D}_{ij}$. If the only relevant terms in (19) are $\tilde{\xi}^U_{11}$ and $\tilde{\xi}^D_{22}$, then they are constrained from the neutral kaon system to be $\lesssim 10^{-2}\sqrt{M_H/{\rm GeV}}$ [5]. With account of (17) this favors the limit

$$|P_{\rm T}(120° < \theta < 160°)| \lesssim 3\times10^{-2}\left(\frac{315\,{\rm GeV}}{M_H}\right)^{3/2}\left(\frac{z}{2\,{\rm GeV}^{-1}}\right) \times\left(\frac{{\rm Im}\left[\tilde{\xi}^U_{11} + \tilde{\xi}^{D*}_{22}\right]}{10^{-2}}\right)\,.$$

It is more than 300 times larger than the expected experimental sensitivity to $P_{\rm T}$ [8]. Note that without special fine-tuning between ${\rm Im}\left[\tilde{\xi}^U_{11}\right]$ and ${\rm Im}\left[\tilde{\xi}^{D*}_{22}\right]$, the strongest limit on $P_{\rm T}$ comes from the search for the transverse muon polarization in $K \to \pi^0\mu\nu$ decay [21], since the interaction (18) generally provides both $G_{\rm P}$ and $G_{\rm S}$ of the same order [18] (see Sect. 4.1), and the latter are multiplied by factors of similar magnitude. This yields

$$|P_{\rm T}(120° < \theta < 160°)| \lesssim 3\times10^{-3}\,,$$

at 95% CL.

On the other hand, for special structures of the mixing matrices $\tilde{\xi}^U$, $\tilde{\xi}^D$, $P_{\rm T}$ in the 2HD model can be as large as 0.1.

5.2 Three-Higgs doublet models

In these models three different Higgs doublets (h_u, h_d, h_l) couple to up- and down-type quarks and leptons, respectively. The relevant interaction between SM fermions and charged Higgs bosons for $K_{\mu 2\gamma}$ decay reads

$$\mathcal{L} = \frac{\sqrt{G_{\rm F}}}{\sqrt[4]{2}}\sum_{i=1}^{2}\{h_i^+[\alpha_i\bar{u}VM_d(1+\gamma_5)d + \beta_i\bar{u}M_uV(1-\gamma_5)d + \gamma_i\bar{\nu}M_l(1+\gamma_5)e]\} + {\rm h.c.}\,, \quad (20)$$

where V is the CKM matrix, M_d, M_u and M_l are diagonal down-type quark, up-type quark and lepton mass matrices, respectively, and α_i, β_i and γ_i ($i = 1, 2$) are complex mixing parameters in the Higgs sector. This interaction results in [18]

$${\rm Im}\Delta_{\rm P} = -\left(\frac{m_K^2}{m_1^2} - \frac{m_K^2}{m_2^2}\right) \times\left({\rm Im}\gamma_1\alpha_1^* - \frac{m_u}{m_s}{\rm Im}\gamma_1\beta_1^*\right)\,, \quad (21)$$

where m_i are the masses of charged Higgs bosons. The current experimental constraints on the parameters of the

theory (see, e.g., [19] for a collection of relevant formulae) give the same order bound on $P_{\rm T}$ as obtained from [21] for $P_{\rm T}$ in $K \to \pi^0\mu\nu$ decay (as far as $G_{\rm P}$ and $G_{\rm S}$ emerging from the Lagrangian (20) are generally of the same order),

$$|P_{\rm T}(120^\circ < \theta < 160^\circ)| \lesssim 3 \times 10^{-3}\,, \quad 95\%\ {\rm CL}\,.$$

This upper limit is about 30 times larger than the expected sensitivity of the new experiment.

5.3 Supersymmetric models with R-parity

In the minimal supersymmetric extension of the Standard Model (MSSM) the relevant four-fermion interactions emerge due to W-boson and charged Higgs boson exchanges with couplings being enhanced by squark–gluino loops.

A right-handed current interaction is generated by the diagram with gluino, stop and sbottom particles running in the loop with left–right mass insertions both for stop and sbottom. This gives rise to the effective interaction [20]

$$\begin{aligned}\mathcal{L}_{\rm I} =& -C\frac{G_{\rm F}}{\sqrt{2}}\bar{s}\gamma^\alpha\left(1+\gamma_5\right)u\cdot\bar{\nu}\gamma_\alpha\left(1-\gamma_5\right)\mu + {\rm h.c.}\,,\\ C =& I_0\frac{m_t m_b\left(A_t-\mu\cot\beta\right)\left(A_b-\mu\tan\beta\right)}{M_{\tilde g}^4}\\ &\times\frac{\alpha_{\rm s}[M_{\rm SUSY}]}{36\pi}V_{31}^{U_{\rm R}}V_{32}^{D_{\rm R}*}V_{33}^{\rm SCKM*}\,,\end{aligned} \tag{22}$$

where A_t and A_b are the soft supersymmetry breaking trilinear terms for stops and sbottoms, μ is the Higgs superfield mixing parameter, $\tan\beta$ is the ratio of the two Higgs vacuum expectation values, $M_{\tilde g}$ is the gluino mass, $V^{U_{\rm R}}$ and $V^{D_{\rm R}}$ are the rotations in the generation space between up-type right-handed squarks and down-type right-handed squarks and corresponding quark partners, respectively; $V^{\rm SCKM}$ is the super CKM matrix associated with W–squark–squark couplings, and I_0 is given by the integral

$$I_0 = \int_0^1 {\rm d}z_1\int_0^{1-z_1}{\rm d}z_2\frac{24 z_1 z_2}{\left(1+\left(\frac{m_{\tilde t}^2}{M_{\tilde g}^2}-1\right)z_1+\left(\frac{m_{\tilde b}^2}{M_{\tilde g}^2}-1\right)z_2\right)^2}\,.$$

For W-boson exchange, the interaction (22) provides the polarization

$$\begin{aligned}&{\rm Im}(\Delta_{\rm A}+\Delta_{\rm V})_W\\ &= -I_0\frac{m_t m_b\left(A_t-\mu\cot\beta\right)\left(A_b-\mu\tan\beta\right)}{M_{\tilde g}^4}\\ &\quad\times\frac{\alpha_{\rm s}[M_{\rm SUSY}]}{18\pi}\frac{{\rm Im}\left[V_{31}^{U_{\rm R}}V_{32}^{D_{\rm R}*}V_{33}^{\rm SCKM*}\right]}{|V_{us}|}\,.\end{aligned} \tag{23}$$

Current experimental constraints on the parameters of the theory [11] lead to

$$|P_{{\rm T}_W}(120^\circ < \theta < 160^\circ)| \lesssim 0.8 \times 10^{-3}\,, \tag{24}$$

where we set $m_{\tilde t} = m_{\tilde b} = M_{\tilde g}/2$, $\tan\beta \simeq 50$, $M_{\tilde g} \simeq A_b \simeq \mu \simeq A_t \simeq 500$GeV, and ${\rm Im}\left[V_{31}^{U_{\rm R}}V_{32}^{D_{\rm R}*}V_{33}^{\rm SCKM*}\right] \simeq 0.5$.

The charged Higgs boson exchange enhanced by gluon–stop–sbottom loops gives rise to the effective interaction [20]

$$\begin{aligned}\mathcal{L}_{\rm II} =& -C_1\frac{G_{\rm F}}{\sqrt{2}}\bar{s}\left(1+\gamma_5\right)u\cdot\bar{\nu}\left(1+\gamma_5\right)\mu\\ &-C_2\frac{G_{\rm F}}{\sqrt{2}}\bar{s}\left(1-\gamma_5\right)u\cdot\bar{\nu}\left(1+\gamma_5\right)\mu + {\rm h.c.}\,,\\ C_1 =& \frac{\alpha_{\rm s}\left[M_{\rm SUSY}\right]}{3\pi}I_1\frac{m_t m_\mu\tan\beta}{M_{H^+}^2}\frac{A_t\cot\beta+\mu}{M_{\tilde g}}\\ &\times V_{31}^{U_{\rm R}}V_{32}^{D_{\rm L}*}V_{33}^{H*},\\ C_2 =& \frac{\alpha_{\rm s}\left[M_{\rm SUSY}\right]}{3\pi}I_1\frac{m_b m_\mu\tan\beta}{M_{H^+}^2}\frac{A_b\tan\beta+\mu}{M_{\tilde g}}\\ &\times V_{31}^{U_{\rm L}}V_{32}^{D_{\rm R}*}V_{33}^{H*},\\ I_1 =& \int_0^1{\rm d}z_1\int_0^{1-z_1}{\rm d}z_2\frac{2}{1+\left(\frac{m_{\tilde t}^2}{M_{\tilde g}^2}-1\right)z_1+\left(\frac{m_{\tilde b}^2}{M_{\tilde g}^2}-1\right)z_2}\,,\end{aligned}$$

where V^H is the mixing in the coupling between the charged Higgs and the up-type right-handed and down-type left-handed squarks, and $V^{U_{\rm L}}$ and $V^{D_{\rm L}}$ are the rotations in the generation space between up-type left-handed squarks and down-type left-handed squarks and the corresponding quark partners, respectively. This results in

$$\begin{aligned}{\rm Im}\Delta_{P_H} =& -\frac{\alpha_{\rm s}\left[M_{\rm SUSY}\right]}{3\pi}I_1\frac{B_0 m_t\tan\beta}{M_{H^+}^2}\frac{A_t\cot\beta+\mu}{M_{\tilde g}}\\ &\times\frac{{\rm Im}\left[V_{31}^{U_{\rm R}}V_{32}^{D_{\rm L}*}V_{33}^{H*}\right]}{|V_{us}|}\\ &-\frac{\alpha_{\rm s}\left[M_{\rm SUSY}\right]}{3\pi}I_1\frac{B_0 m_b\tan\beta}{M_{H^+}^2}\frac{A_b\tan\beta+\mu}{M_{\tilde g}}\\ &\times\frac{{\rm Im}\left[V_{31}^{U_{\rm L}}V_{32}^{D_{\rm R}*}V_{33}^{H*}\right]}{|V_{us}|}\,.\end{aligned} \tag{25}$$

With the estimate

$${\rm Im}\left[V_{31}^{U_{\rm R}}V_{32}^{D_{\rm L}*}V_{33}^{H*}\right] \simeq 0.5 \ \text{ and } \ {\rm Im}\left[V_{31}^{U_{\rm L}}V_{32}^{D_{\rm R}*}V_{33}^{H*}\right] \simeq 0.5$$

and the same settings as listed below (24) both terms in (25) are of the order 10^{-2}.

So $P_{{\rm T}_W}$ and $P_{{\rm T}_H}$ are 10 and 100 times larger, respectively, than the expected experimental sensitivity.

Note in passing that without a special cancellation associated with the light superpartners, the charged Higgs boson gives a large contribution to $b \to s\gamma$. This yields the bound $M_H > 315\,{\rm GeV}$ [16], which decreases the upper limit on $P_{{\rm T}_H}$ by an order of magnitude.

5.4 Supersymmetric models without R-parity

In this section we consider the supersymmetric extensions of the Standard Model with the violation of the R-parity and the lepton number. The relevant superpotential is given by

$$\mathcal{W}_{\rm RV} = \frac{1}{2}\lambda_{ijk}L_iL_jE_k^c + \lambda'_{ijk}L_iQ_jD_k^c$$

with L_i and E_i^c being the chiral superfields of the lepton doublets and singlets, and Q_i, D_i^c denote the chiral superfields of the quark doublets and down-type singlets, respectively. In this model the contribution to $K_{\mu 2\gamma}$ decay arises due to the interaction

$$\mathcal{L}_{\rm RV} = -\frac{\lambda^*_{2i2}\lambda'_{i12}}{4M^2_{\tilde{e}_{\rm L_i}}}\bar{s}(1-\gamma_5)u\cdot\bar{\nu}(1+\gamma_5)\mu\,,$$

where $M_{\tilde{e}_{\rm L_i}}$ are the masses of the left-handed sleptons. The resulting transverse muon polarization reads [5]

$$\mathrm{Im}\Delta_{\rm P} = \mathrm{Im}\left[\lambda^*_{2i2}\lambda'_{i12}\right]\frac{B_0}{m_\mu|V_{us}|}\frac{1}{2\sqrt{2}G_{\rm F}M^2_{\tilde{e}_{\rm L_i}}}\,. \qquad (26)$$

The strongest relevant experimental limit on the parameters of the model comes from the measurement of $K_{\rm L}\to\bar{\mu}\mu$ decay rate [22], and one can obtain from (17) and (26):

$$\begin{aligned}&|P_{\rm T}(120^\circ<\theta<160^\circ)|\\ &\lesssim 1.5\times10^{-5}\left(\left(\frac{\mathrm{Im}\left[\lambda^*_{212}\lambda'_{112}\right]}{3.8\times10^{-7}}\right)\left(\frac{M_{\tilde{\nu}_1}}{M_{\tilde{e}_{\rm L_1}}}\right)^2\right.\\ &\qquad\left.+\left(\frac{\mathrm{Im}\left[\lambda^*_{232}\lambda'_{312}\right]}{3.8\times10^{-7}}\right)\left(\frac{M_{\tilde{\nu}_3}}{M_{\tilde{e}_{\rm L_3}}}\right)^2\right)\,,\end{aligned} \qquad (27)$$

with the $M_{\tilde{\nu}_i}$ being sneutrino masses. This contribution, (27), is obviously too small to be detected. Note in passing that in models with the relevant hierarchy in the slepton sector or in models with some cancellation of the sparticle contributions to $K_{\rm L}\to\bar{\mu}\mu$ decay, one could expect $P_{\rm T}$ in $K_{\mu 2\gamma}$ at the level of 10^{-3}.

5.5 Left–right symmetric models

In models with left–right gauge symmetries $SU(2)_{\rm L}\times SU(2)_{\rm R}\times U(1)_{B_{\rm L}}$ [23] the four-fermion interaction which contributes to $K_{\mu 2\gamma}$ decay is given by

$$\mathcal{L}_{\rm LR} = -\frac{G_{\rm F}}{\sqrt{2}}\left(\frac{g_{\rm R}}{g_{\rm L}}\right)\xi V^{\rm R*}_{us}\bar{s}\gamma_\mu(1+\gamma_5)u\cdot\bar{\nu}\gamma^\mu(1-\gamma_5)\mu\,,$$

where ξ is the left–right complex mixing parameter, $V^{\rm R}$ is the right-handed CKM matrix and $g_{\rm L,R}$ are the coupling constants of $SU(2)_{\rm L}$ and $SU(2)_{\rm R}$, respectively. This interaction results [5] in

$$\mathrm{Im}(\Delta_{\rm A}+\Delta_{\rm V}) = 2\frac{g_{\rm R}}{g_{\rm L}}\mathrm{Im}\left(\xi V^{R*}_{us}\right)\,. \qquad (28)$$

With the current experimental constraints on the parameters of the theory [24] one can obtain from (16) and (28)

$$\begin{aligned}&|P_{\rm T}(120^\circ<\theta<160^\circ)|\\ &\lesssim 2\times10^{-3}\left(\frac{g_{\rm R}/g_{\rm L}}{1}\right)\mathrm{Im}\left[\left(\frac{\xi}{0.033}\right)\left(\frac{V^{R*}_{us}}{|V_{us}|}\right)\right]\,,\end{aligned}$$

which is 20 times larger than the expected statistical uncertainty of $P_{\rm T}$ (12).

5.6 Leptoquark models

There exist two leptoquark models contributing to $P_{\rm T}$ in $K_{\mu 2\gamma}$ decay. The quantum numbers of the leptoquarks under the Standard Model group are

$$\phi_1 = \left(3,2,\frac{7}{3}\right)\,,\quad\text{(Model I)}\,,$$

$$\phi_2 = \left(3,1,-\frac{2}{3}\right)\,,\quad\text{(Model II)}\,,$$

and the general couplings involving these leptoquarks are given by

$$\mathcal{L}_{\rm LQ_I} = \left(\frac{\lambda_1}{2}\bar{Q}\,(1+\gamma_5)\,e + \frac{\lambda'_1}{2}\bar{u}\,(1-\gamma_5)\,L\right)\phi_1 + \text{h.c.}\,,$$

$$\mathcal{L}_{\rm LQ_{II}} = \left(\frac{\lambda_2}{2}\bar{Q}\,(1+\gamma_5)\,L^c + \frac{\lambda'_2}{2}\bar{u}\,(1-\gamma_5)\,e^c\right)\phi_2 + \text{h.c.}$$

The relevant terms read

$$\mathcal{L}^{K\mu\nu}_{\rm LQ_I} = \frac{\lambda^{22}_1\lambda'^{1i*}_1}{4M^2_{\phi_1}}\bar{s}\,(1+\gamma_5)\,\mu\cdot\bar{\nu}_i\,(1+\gamma_5)\,u + \text{h.c.}\,,$$

$$\mathcal{L}^{K\mu\nu}_{\rm LQ_{II}} = \frac{\lambda^{2i}_2\lambda'^{12*}_2}{4M^2_{\phi_2}}\bar{s}\,(1+\gamma_5)\,\nu^c_i\cdot\bar{\mu}^c\,(1+\gamma_5)\,u + \text{h.c.}\,,$$

where the M_{ϕ_1} are the leptoquark masses, and they yield [5]

$$\mathrm{Im}\Delta_{P_{\rm I}} = -\mathrm{Im}\left[\lambda^{22}_1\lambda'^{1i*}_1\right]\frac{B_0}{m_\mu|V_{us}|}\frac{\sqrt{2}}{8G_{\rm F}M^2_{\phi_1}}\,, \qquad (29)$$

$$\mathrm{Im}\Delta_{P_{\rm II}} = -\mathrm{Im}\left[\lambda^{2i}_2\lambda'^{12*}_2\right]\frac{B_0}{m_\mu|V_{us}|}\frac{\sqrt{2}}{8G_{\rm F}M^2_{\phi_2}}\,. \qquad (30)$$

With the current experimental constraints on the parameters of the models with leptoquarks, the strongest limit on $P_{\rm T}$ comes from the measurement of the $P_{\rm T}$ in $K\to\pi^0\mu\nu$ decay [21] (supposing that the $G_{\rm P}$ and $G_{\rm S}$ constants are generally of the same order in this theory), and this yields

$$|P_{\rm T}(120^\circ<\theta<160^\circ)|\lesssim 3\times10^{-3}$$

at 95% CL. This bound is larger than the expected experimental sensitivity by a factor of 30.

6 Conclusions

The analysis presented in this paper concerns the information which could be drawn from the experiment of the measurement of the transverse muon polarization $P_{\rm T}$ in $K \to \mu\nu\gamma$ decay.

It was found that the FSI $P_{\rm T}$ distribution over the Dalitz plot is sensitive to the values of the kaon form factors. The best sensitivity is exhibited in the region of large angles θ between muon and photon. The $P_{\rm T}$ calculated in this region allows one to pin down the signs of the kaon form factors in spite of the uncertainties associated with the unknown dependence of the form factors on the momentum of the lepton pair. To this end the statistics of $\geq 10^9$ $K_{\mu 2\gamma}$ events with large $\theta > 120^\circ$ is required.

It was recently demonstrated [13] that the normal muon polarization $P_{\rm N}$ is very sensitive to the signs and the values of the kaon form factors. Since $P_{\rm N}$ emerges at tree level, the statistics expected in the new experiment proposed at JHF allows one to determine for sure the kaon form factors with a few percent accuracy. The unknown dependence of the form factors on the momentum of the lepton pair should be determined by fitting the experimental data on the $P_{\rm N}$ Dalitz plot distribution.

Finally, it was shown that possible new physics contributions and the FSI contribution to $P_{\rm T}$ show different behaviors over the Dalitz plot. In particular, at large θ the new physics contributions to $P_{\rm T}$ grow by one and a half order of magnitude, which suggests one to consider this region as the most interesting to probe the new physics responsible for T-violating effects. In most cases the contribution from new physics can exceed the measurable level of $P_{\rm T}$ by one or two orders of magnitude. Moreover, the extraction of form factor values from $P_{\rm N}$ allows the background contribution from FSI to the non-SM T-violating muon polarization to be determined with a small uncertainty.

It is worth to note that the signs of pion form factors $F_{\rm V}^\pi$ and $F_{\rm A}^\pi$ have not been measured yet [11]. The experimental situation there is similar to the one for kaons, though $F_{\rm V}^\pi$ has a definite CVC prediction and the pion form factors are almost constants over the whole Dalitz plot. The FSI contributions to $P_{\rm T}$ are of the order of 10^{-4} (10^{-3}) for $\pi_{\mu 2\gamma}$ ($\pi_{e2\gamma}$) [25]. From the analysis given above, we can suggest that the measurement of the transverse lepton polarization in $\pi_{l2\gamma}$ would allow us to pin down the signs of the pion form factors, if possible contributions to $P_{\rm T}$ from physics beyond the Standard Model are negligible. This issue will be considered elsewhere.

Acknowledgements. This work is supported in part by RFBR grant 02-02-17398 and by the program SCOPES of the Swiss National Science Foundation, project No. 7SUPJ062239. The work of F.B. is supported in part by CRDF grant RP1-2364-MO-02. The work of D.G. is supported in part by the INTAS YSF 2001/2-142.

References

1. T.D. Lee, Phys. Rev. D **8**, 1226 (1973)
2. S. Weinberg, Phys. Rev. D **42**, 860 (1990); R. Garisto, G.L. Kane, Phys. Rev. D **44**, 2038 (1991); G. Belanger, C.Q. Geng, Phys. Rev. D **44**, 2789 (1991); G.H. Wu, J.N. Ng, Phys. Lett. B **392**, 93 (1997) [hep-ph/9609314]
3. E. Gabrielli, Phys. Lett. B **301**, 409 (1993)
4. J. Bijnens, G. Ecker, J. Gasser, Nucl. Phys. B **396**, 81 (1993) [hep-ph/9209261]
5. C.H. Chen, C.Q. Geng, C.C. Lih, Phys. Rev. D **56**, 6856 (1997) [hep-ph/9709447]
6. M. Abe et al. [KEK-E246 Collaboration], Phys. Rev. Lett. **83**, 4253 (1999)
7. Y.G. Kudenko, Phys. Atom. Nucl. **65**, 244 (2002) [Yad. Fiz. **65**, 269 (2002)] [hep-ex/0103007]
8. Y.G. Kudenko, A.N. Khotyantsev, Phys. Atom. Nucl. **63**, 820 (2000) [Yad. Fiz. **63**, 890 (2000)]; Yu. Kudenko, Measurement of T-violation in K^+ decays at JHF, Proceedings of the International Workshop on JHF Science, March 4–7, 1998, Tsukuba, Japan, Vol. II, p. 39
9. M. Furusaka et al., The Joint Project for High-Intensity Proron Accelerators, KEK Report 99-4, 1999
10. S.C. Adler et al. [E787 Collaboration], Phys. Rev. Lett. **85**, 2256 (2000) [hep-ex/0003019]
11. K. Hagiwara et al. [Particle Data Group Collaboration], Phys. Rev. D **66**, 010001 (2002)
12. A.A. Poblaguev et al., Phys. Rev. Lett. **89**, 061803 (2002) [hep-ex/0204006]
13. F.L. Bezrukov, D.S. Gorbunov, Y.G. Kudenko, Phys. Rev. D **67**, 091503 (2003) [hep-ph/0302106]
14. D.Y. Bardin, E.A. Ivanov, Sov. J. Part. Nucl. **7**, 286 (1976) [Fiz. Elem. Chast. Atom. Yadra **7**, 726 (1976)]
15. V.V. Braguta, A.E. Chalov, A.A. Likhoded, Phys. Rev. D **66**, 034012 (2002) [hep-ph/0205203]
16. P. Gambino, M. Misiak, Nucl. Phys. B **611**, 338 (2001) [hep-ph/0104034]
17. V.D. Barger, J.L. Hewett, R.J. Phillips, Phys. Rev. D **41**, 3421 (1990)
18. M. Kobayashi, T.T. Lin, Y. Okada, Prog. Theor. Phys. **95**, 361 (1996) [hep-ph/9507225]
19. Y. Grossman, Nucl. Phys. B **426**, 355 (1994) [hep-ph/9401311]
20. G.H. Wu, J.N. Ng, Phys. Rev. D **55**, 2806 (1997) [hep-ph/9610533]
21. M. Abe et al., hep-ex/0211049
22. D. Choudhury, P. Roy, Phys. Lett. B **378**, 153 (1996) [hep-ph/9603363]
23. J.C. Pati, A. Salam, Phys. Rev. D **10**, 275 (1974); R.N. Mohapatra, J.C. Pati, Phys. Rev. D **11**, 566 (1975); R.N. Mohapatra, J.C. Pati, Phys. Rev. D **11**, 2558 (1975); G. Senjanovic, R.N. Mohapatra, Phys. Rev. D **12**, 1502 (1975)
24. G. Barenboim, J. Bernabeu, J. Prades, M. Raidal, Phys. Rev. D **55**, 4213 (1997) [hep-ph/9611347]
25. F.L. Bezrukov, D.S. Gorbunov, Phys. Rev. D **66**, 054012 (2002) [hep-ph/0205158]